Large aperture PPMgLN based high-power optical parametric oscillator at 3.8 μm pumped by a nanosecond linearly polarized fiber MOPA

Dejiao Lin,[1] Shaif-ul Alam,[1] Yonghang Shen,[2] Tao Chen,[2] Bo Wu,[2] and David J. Richardson[1,*]

[1]*Optoelectronic Research Centre, University of Southampton, Southampton SO17 1BJ, UK*
[2]*State Key Laboratory of Modern Optical Instrumentation, Zhejiang University, Hangzhou 310027, China*
[*]*djr@orc.soton.ac.uk*

Abstract: We report a large aperture PPMgLN based OPO generating 21W of average output power at a slope efficiency of 45%. The OPO is pumped with the output from a polarization maintaining Ytterbium doped fiber MOPA operating at 1060nm producing 20ns pulses at a repetition rate of 100kHz and an average output power of 58W (after the isolators). A maximum of 5.5W of optical power was recorded at the idler wavelength of 3.82μm without thermal roll-off. The pulse rise/fall time plays a significant role in the OPO conversion efficiency and that further enhancements in the efficiency should be possible using pulses with faster rise and fall times.

OCIS codes: (190.4970) Parametric oscillators and amplifiers; (060.2320) Fiber optics amplifiers and oscillators; (320.5540) Pulse shaping.

References and links

1. K. P. Petrov, L. Goldberg, W. K. Burns, R. F. Curl, and F. K. Tittel, "Detection of CO in air by diode-pumped 4.6-μm difference-frequency generation in quasi-phase-matched $LiNbO_3$," Opt. Lett. **21**(1), 86–88 (1996).
2. W. R. Bosenberg, A. Drobshoff, J. I. Alexander, L. E. Myers, and R. L. Byer, "93% pump depletion, 3.5-W continuous-wave, singly resonant optical parametric oscillator," Opt. Lett. **21**(17), 1336–1338 (1996).
3. L. E. Myers and W. R. Bosenberg, "Periodically poled lithium niobate and quasi-phase-matched optical parametric oscillators," IEEE J. Quantum Electron. **33**(10), 1663–1672 (1997).
4. H. Ishizuki and T. Taira, "High-energy quasi-phase-matched optical parametric oscillation in a periodically poled $MgO:LiNbO_3$ device with a 5 mm×5 mm aperture," Opt. Lett. **30**(21), 2918–2920 (2005).
5. B. Wu, J. Kong, and Y. Shen, "High-efficiency semi-external-cavity-structured periodically poled MgLN-based optical parametric oscillator with output power exceeding 9.2 W at 3.82 microm," Opt. Lett. **35**(8), 1118–1120 (2010).
6. D. J. Richardson, J. Nilsson, and W. A. Clarkson, "High power fiber lasers: current status and future perspectives [Invited]," J. Opt. Soc. Am. B **27**(11), B63–B92 (2010).
7. P. E. Britton, D. Taverner, K. Puech, D. J. Richardson, P. G. R. Smith, G. W. Ross, and D. C. Hanna, "Optical parametric oscillation in periodically poled lithium niobate driven by a diode-pumped, Q-switched erbium fiber laser," Opt. Lett. **23**(8), 582–584 (1998).
8. C. Avila, R. Burnham, Y. Chen, W. Torruellas, H. Verdun, and R. Utano, "Polarization maintaining master oscillator fiber amplifier (MOFA) for high repetition rate applications," Proc. SPIE **5335**, 24–32 (2004).
9. S. Chaitanya Kumar, R. Das, G. K. Samanta, and M. Ebrahim-Zadeh, "Optimally-output-coupled, 17.5 W, fiber-laser-pumped continuous-wave optical parametric oscillator," Appl. Phys. B **102**(1), 31–35 (2011).
10. D. W. Chen and T. S. Rose, "Low noise 10-W CW OPO generation near 3 μm with MgO doped PPLN," Conference on Lasers and Electro-Optics (CLEO) **1-3**, 1829–1831 (2005).
11. Y. Shen, S.- Alam, K. Kang Chen, D. Lin, S. Cai, B. Wu, P. Jiang, A. Malinowski, and D. J. Richardson, "PPMgLN-Based High-Power Optical Parametric Oscillator Pumped by Yb3+-Doped Fiber Amplifier Incorporates Active Pulse Shaping," IEEE J. Sel. Top. Quantum Electron. **15**(2), 385–392 (2009).
12. A. Malinowski, K. T. Vu, K. K. Chen, J. Nilsson, Y. Jeong, S. U. Alam, D. Lin, and D. J. Richardson, "High power pulsed fiber MOPA system incorporating electro-optic modulator based adaptive pulse shaping," Opt. Express **17**(23), 20927–20937 (2009).
13. D. Lin, S. U. Alam, P. S. Teh, K. K. Chen, and D. J. Richardson, "Selective excitation of multiple Raman Stokes wavelengths (green-yellow-red) using shaped multi-step pulses from an all-fiber PM MOPA," Opt. Express **19**(3), 2085–2092 (2011).

#165617 - $15.00 USD Received 30 Mar 2012; revised 9 May 2012; accepted 6 Jun 2012; published 20 Jun 2012

14. D. Lin, S. U. Alam, A. Malinowski, K. K. Chen, J. R. Hayes, J. C. Flannagan, V. Geddes, J. Nilsson, S. Ingram, S. Norman, and D. J. Richardson, "Temporally and spatially shaped fully-fiberized ytterbium-doped pulsed MOPA," Laser Phys. Lett. **8**(10), 747–753 (2011).
15. B. Wu, Y. Shen, and S. Cai, "Widely tunable high power OPO based on a periodically poled MgO doped lithium niobate crystal," Opt. Laser Technol. **39**(6), 1115–1119 (2007).
16. A. Henderson and R. Stafford, "Spectral broadening and stimulated Raman conversion in a continuous-wave optical parametric oscillator," Opt. Lett. **32**(10), 1281–1283 (2007).
17. Z. Sacks, O. Gayer, E. Tal, and A. Arie, "Improving the efficiency of an optical parametric oscillator by tailoring the pump pulse shape," Opt. Express **18**(12), 12669–12674 (2010).
18. O. Gayer, Z. Sacks, E. Galun, and A. Arie, "Temperature and wavelength dependent refractive index equations for MgO-doped congruent and stoichiometric LiNbO3," Appl. Phys. B **91**(2), 343–348 (2008).

1. Introduction

High power optical parametric oscillators (OPO) operating in the mid-infrared (IR) wavelength range (3–5 μm) are desirable for a wide range of applications including spectroscopy, environmental monitoring, LIDAR and missile counter-measures [1,2]. Quasi-phase-matched (QPM) OPOs based on periodically poled magnesium-oxide doped lithium niobate (PPMgLN) have moved into the mainstream of OPO research due to the large effective nonlinear coefficient, excellent power handling characteristics and wide transparency range of PPMgLN crystals [3–5]. High efficiency and high power PPMgLN based OPOs pumped by bulk solid state pump sources have been extensively investigated [2–5]. Fiber laser pumped OPOs represent a new generation of compact, high power parametric devices due to the excellent beam quality, simple thermal management schemes and ultrahigh electrical-optical conversion efficiencies of such pump sources [6–10]. The highest reported mid-IR power so far from a fiber pumped OPO is 10 W operating at 2.94 μm pumped by a 50 W continuous wave Yb doped fiber laser operating with a tightly focused beam waist of 70 μm [10]. However, when the mid-IR is generated at longer wavelengths, especially at wavelengths exceeding 3.5 μm, a much larger beam size is required so as to overcome the stronger thermal-lensing effects due to the higher idler absorption. In order to keep high pump intensities and to retain high OPO conversion efficiencies at these wavelengths pulsed fiber lasers with high peak powers become the favored form of pump source.

We have previously reported a pulsed fiber master oscillator power amplifier (MOPA) pumped OPO based on a 50 mm × 1 mm × 1 mm PPMgLN crystal [11]. An overall OPO output power of 11 W (with 2.7 W of idler power at 3.5 μm) was achieved pumped by a 28 W MOPA. In the work reported herein we significantly improved the MOPA performance in terms of higher output peak power by adopting a shorter amplifier fiber (using a fiber with a stronger cladding pump absorption) and greater stability by using a fully polarization maintaining (PM) fiberized system. Moreover, we designed and fabricated a larger aperture PPMgLN wafer which allows for a relatively large focused beam waist which helps to reduce thermal-lens effects. Using adaptive pulse shaping of the seed diode [12,13] we demonstrate a reduction in the impact of dynamic gain saturation and optical Kerr/Raman nonlinearities [14] within the fiber MOPA, obtaining shaped signal and idler pulses at the OPO output. A total OPO power output of 21 W with an idler power of 5.5 W at 3.8 μm were obtained at a pump power of 58 W, with no sign of thermal roll-off indicating considerable scope for further power scaling.

2. System setup

A schematic diagram of the all-fiber PM MOPA and the OPO system is illustrated in Fig. 1. The MOPA was seeded by a fiber pigtailed Fabry-Perot laser diode (Bookham CPE425) wavelength stabilized at 1060 nm with an external fiber Bragg grating. The diode was modulated by a Stanford pulse generator to deliver rectangular shaped output pulses with adjustable repetition rate and a selectable pulse duration ranging from a few ns to hundreds of ns. The seed laser output passed through an in-line electro-optic modulator (EOM), which was driven by an arbitrary waveform generator (AWG) with 4ns feature definition triggered by the

#165617 - $15.00 USD Received 30 Mar 2012; revised 9 May 2012; accepted 6 Jun 2012; published 20 Jun 2012

Stanford pulse generator. The AWG waveform applied to the EOM was designed to produce rectangular shaped pulses at the amplifier output in the presence of dynamic gain saturation within the fiber MOPA and to minimize the impact of optical Kerr/Raman nonlinearities. We chose to use an EOM for pulse shaping rather than direct modulation of the diode drive current itself as this provided a faster shaping capability. The seed signal from the EOM was amplified by an all-fiber, three-stage PM amplifier chain to deliver single mode, single polarization output.

The first pre-amplifier (bi-directional core pumped) delivered 30 mW of average output power whilst the second pre-amplifier (double clad counter pumped) produced 200 mW of average output power and both the stages were identical to those described in Ref [13], whereas the fiber of the final stage amplifier in this case was a large mode area (LMA), PM, double-clad active fiber (Nufern PLMA-YDF-25/250). The fiber has a core diameter of 25 µm and a core NA of 0.06. The cladding diameter of the polymer coated fiber was 250 µm with a cladding NA of 0.45. The measured cladding absorption of the fiber at the pump wavelength (975 nm) was 5.1 dB/m. A 3.8 m length of this fiber was chosen such that the amplifier not only provides optimum signal gain but also absorbs most of the launched pump power. To minimize the splice loss between the passive single-mode PM fiber and the LMA active fiber the outer diameter of the LMA fiber was tapered down to 90 µm and a core diameter of 9 µm during splicing. This helps to reduce the mode field diameter mismatch between the two dissimilar fibers ensuring a lower splice loss. Moreover tapering, in conjunction with winding the fiber around an aluminum spool with a coil diameter of 80mm, allowed us to obtain robust single mode operation even though the active fiber core can support several transverse modes. A 2 mm long pure silica mode-expanding end-cap was spliced to the end of the fiber to reduce the laser intensity at the fiber facet. The end cap was angle polished to avoid retro-reflection back into the fiber core. The amplifier was end-pumped using a 975 nm diode stack. A simple lens combination was used to achieve ~80% coupling efficiency into the fiber. A dichroic mirror was used to split the pump and signal output.

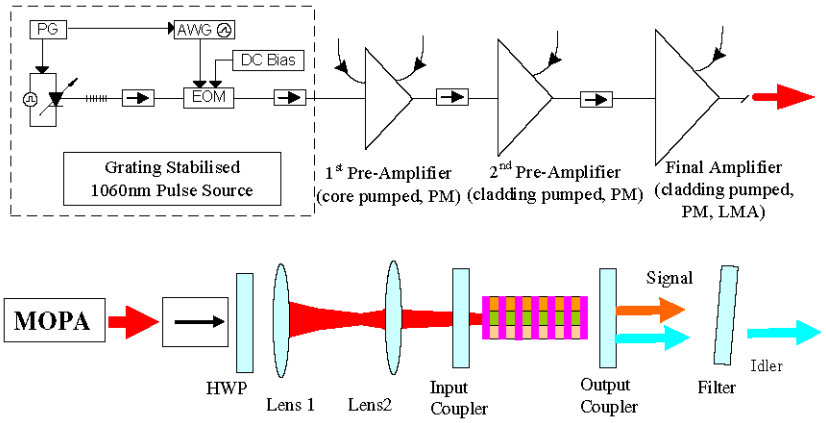

Fig. 1. Schematic of the Yb-doped all-fiber PM MOPA and PPMgLN based OPO system.

The collimated output beam from the MOPA was passed through a pair of telescopic lenses and focused into the PPMgLN crystal for OPO generation. Two back-to-back bulk isolators were used to safeguard the fiber amplifier chain from any unwanted reflections. The total pump loss through this back-to-back isolator combination was about 1 dB. The polarization of the MOPA output was rotated by a half wave plate (HWP) to align to the principal axis of the PPMgLN crystal for maximum OPO conversion efficiency. By choosing different combinations of focal length lenses we could set the required focused beam waist within the crystal. In our experiment we chose a beam waist of ~1.2 mm corresponding to a

#165617 - $15.00 USD Received 30 Mar 2012; revised 9 May 2012; accepted 6 Jun 2012; published 20 Jun 2012

long Rayleigh length of ~1 m. This allowed us to use plane cavity mirrors which are much more convenient in terms of alignment compared to the use of curved mirrors. The input mirror was anti-reflection coated across the 1.06 μm band and had a high reflectivity from 1.4 μm to 1.6 μm as well as from 3.5 μm to 4.0 μm. The output coupler had a high reflectivity coating across the 1.06 μm band and exhibited high transmission between 3.5 μm to 4.0 μm. The reflectivity of the output coupler at 1.47 μm was 55%. The PPMgLN crystal used was a home made wafer [15] with MgO concentration of 5%, a uniform homogeneous domain reverse period of 29.4 μm and a channel size of 50 mm × 2 mm × 2 mm. Both ends of the crystal were finely polished and were anti-reflection coated at wavelengths of 1.06 μm, 1.4 μm to 1.6 μm and 3.5 μm to 4.0 μm. The air gap between the cavity mirrors and the crystal was just 1 mm on both sides. A filter with high reflectivity at the signal wavelengths was used to block the OPO signal so that the idler power could be measured separately.

3. Experimental results

The impact of the peak power of the pump pulses and the focused beam size in the PPLN crystal on the OPO conversion efficiency were first investigated. To do this we fixed the pump pulse repetition rate at 100 kHz and investigated the OPO performance as we varied the pump pulse duration at fixed pump spot size (1.2 mm diameter). Changing the pulse duration at a fixed average output power ensures the peak power scales with the pulse duty cycle. We chose pulse durations of 100 ns, 48 ns, 24 ns and 20 ns respectively (corresponding to the duty cycles of 100, ~200, ~400 and 500). The results are summarized in Fig. 2. It is observed that the higher the pump peak power the better the OPO conversion efficiency. Reducing the repetition rate whilst maintaining the pulse width could also in principle be used to increase the peak power, however the build up of strong amplified spontaneous emission (ASE) in the 1030-1040 nm region at high MOPA output powers limited our capability to this option.

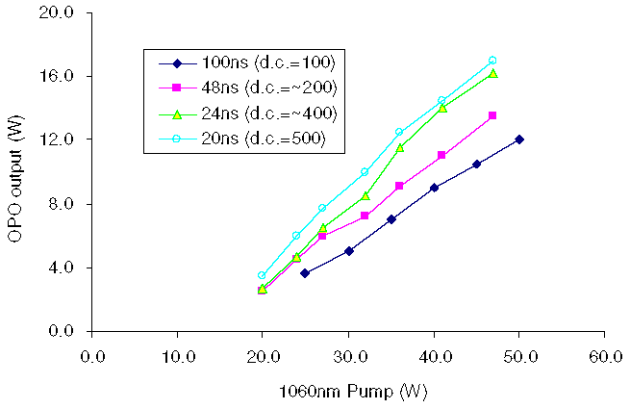

Fig. 2. OPO Output powers as a function of 1060 nm pump power at various average pump power levels. The pulse peak power is obtained by multiplying the average power by the corresponding duty cycle (d.c.).

In Fig. 3 we show the OPO performance for different focused beam sizes (1.2 mm vs. 0.9 mm) for the same pump pulse conditions (100 kHz, 20 ns). When the average pump power was relatively low, the OPO conversion efficiency for smaller beam waist (higher intensity) was higher than that with larger beam waist. However, when the average pump power exceeded 40 W a clear roll-off in OPO power (pink curve in Fig. 3(a)) can be observed which we believe to be due to the temperature increases/thermal gradients within the PPMgLN crystal driven by idler absorption that affects the phase matching conditions – evidence in support of this postulate is provided by the shifting and broadening of the OPO signal spectrum [16] observed in Fig. 3(b). Therefore for a given pump peak power one has to optimize the beam waist on the crystal to maximize the OPO output.

#165617 - $15.00 USD Received 30 Mar 2012; revised 9 May 2012; accepted 6 Jun 2012; published 20 Jun 2012

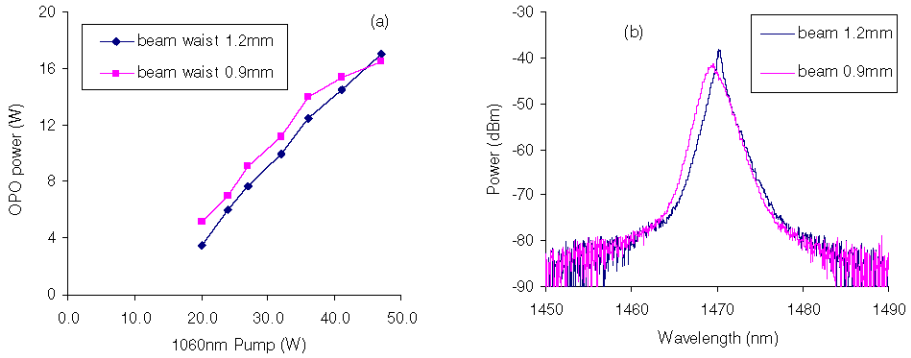

Fig. 3. (a) Output power and (b) signal spectra of the OPO with regard to varied beam waist size (47W pump power).

Based on these initial trials, a beam waist of 1.2 mm was chosen for the MOPA operating at a repetition rate of 100 kHz and a pulse duration of 20 ns. These settings allowed us to achieve relatively high peak power pulses without a strong accompanying ASE component. A maximum average (peak) output power of 76 W (38 kW) with a polarization extinction ratio of 13 dB and good beam quality ($M^2 < 1.1$) was obtained from the fiber MOPA. Figure 4(a) shows the spectra at the output of the final stage amplifier for three different output powers with square shaped optical output pulses. The 3 dB spectral bandwidth of the laser output broadened slightly from 0.2 nm to 0.4 nm at the highest pulse energies used in our OPO experiments. The ASE at 1040 nm and the stimulated Raman scattering (SRS) at 1115 nm were 25 dB and 40 dB lower than the signal peak respectively at the highest operating peak power.

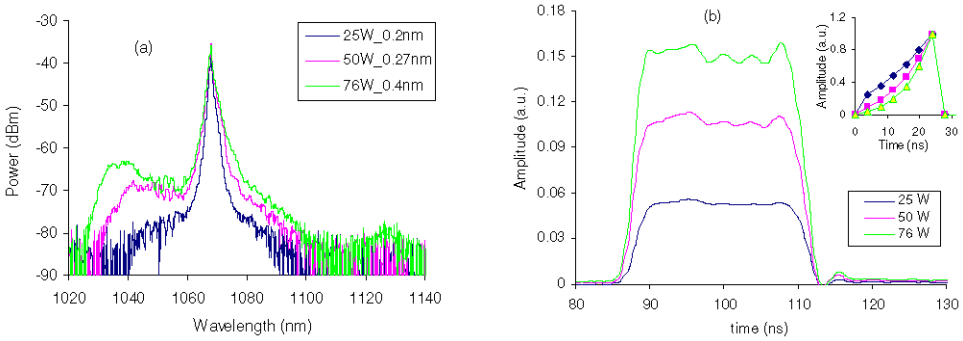

Fig. 4. (a) Spectra and (b) pulse shapes of the MOPA output for various output powers.

Although in principle it is helpful to use a shaped pulse with a relatively strong peak power close to the leading edge in order to reduce the OPO threshold [17], we found when trying this experimentally that the OPO conversion efficiency was not improved when the overall pump power (and signal peak power) was high. Accordingly to preserve the spectral integrity and minimize SRS without compromising the pulse energy, the initial pulses were pre-shaped to obtain square output pulses from our MOPA system. The pulse shapes at different power levels are shown in Fig. 4(b) (the inset shows the corresponding pre-shaped pulses from the seed diode).

Although a maximum average output power of 76 W was available at the output of the MOPA the output power was reduced to 58 W (single polarization) after passing through the isolators and the M^2 was degraded to 1.2. Figure 5 plots the signal, idler and the total OPO output powers as a function of the pump power. The threshold average power for the OPO was measured to be ~15 W corresponding to a peak power of ~7.5 kW. Altogether 21 W of

#165617 - $15.00 USD Received 30 Mar 2012; revised 9 May 2012; accepted 6 Jun 2012; published 20 Jun 2012

OPO output power was obtained at a slope efficiency of 45% of which 5.5W power was measured at the idler wavelength of 3.82 µm at a slope efficiency of 13%, which could be higher if a more optimal cavity design was adopted [5]. The M^2 of the OPO signal at the maximum output power was measured to be 1.4 which was slightly worse than the pump beam and is believed to be due to thermal effects caused by idler absorption within the PPMgLN crystal. The OPO power was stable to about 3% (standard deviation and measured over a period of 30 minutes). We attribute this power variation to temperature drift of the chiller used to cool the final stage pump source of the MOPA and thermally induced polarization degradation originating within the isolators. No roll-off in output power was observed indicating that further power scaling may be possible with the availability of higher pump power. This signifies the importance of using a large-aperture PPLN crystal to scale up the OPO output power.

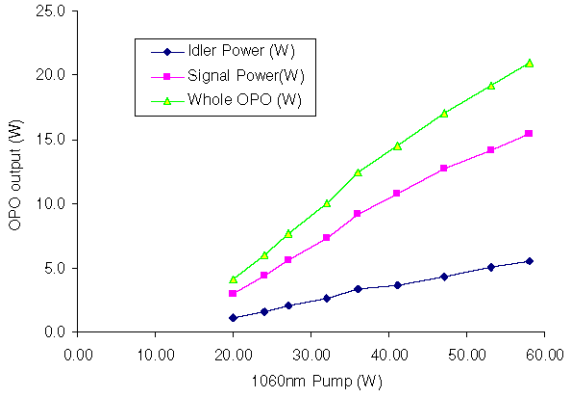

Fig. 5. Output power dependence of the OPO on 1060nm pump coupled into the PPMgLN.

As is shown in Fig. 6(a), the OPO signal wavelength was increasingly red-shifted with increasing pump power. This can be attributed to internal heating within the PPMgLN crystal due to the relatively high absorption of PPMgLN within the idler wavelength band. The internal heating causes both thermal expansion and a change in refractive index of the crystal resulting in an increase in the PPMgLN crystal grating pitch and the observed red-shift in wavelength of the OPO signal. The shift in wavelength is observed to be average idler power dependent – implying that the internal heating of the crystal may be associated with the higher idler intensity. It is possible to estimate the rise in internal temperature of the PPMgLN crystal from the observed wavelength shift. Our calculations indicate that the internal temperatures rose by about 25°C as the average pump power increased from 20 W to 58 W [18]. The 3 dB spectral bandwidth was measured to be less than 0.5 nm at the highest operating power. Figure 6(b) illustrates the OPO signal pulse shapes at different power levels. The OPO takes a long time to build-up at relatively low pump pulse peak power resulting in low conversion efficiency. At high pump pulse peak power the OPO build-up time was reduced to about 4 ns: similar to the rise time of the pump pulse. However as the peak power of the pump pulse increased, the leading edge of the signal pulse sharpened as compared to the trailing edge - similar to that frequently observed with gain saturated amplified optical pulses. Since the OPO build-up time depends on the rise time of the pump pulse this implies that the OPO conversion efficiency might be further increased by adopting a faster AWG so as to reduce the rise/fall times of the pump pulse. Our calculations indicate that close to 20% improvement in conversion efficiency might be possible for 20ns pulses with reduced rise/fall times of ~0.1 ns.

#165617 - $15.00 USD Received 30 Mar 2012; revised 9 May 2012; accepted 6 Jun 2012; published 20 Jun 2012

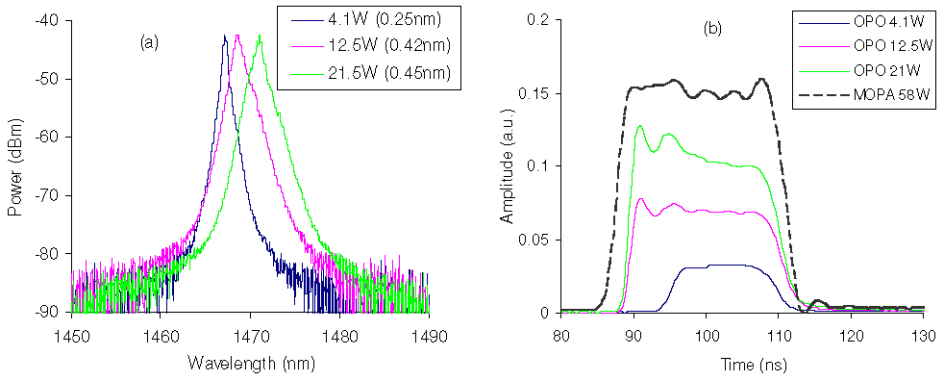

Fig. 6. (a) Spectra and (b) pulse shapes of the OPO signal for various pump powers.

4. Conclusions

In summary, we demonstrate a single polarisation Ytterbium doped fiber MOPA at 1060 nm delivering 76 W of average output power, corresponding to a peak power of 38kW (58W and 29kW after the isolators). The linearly polarized output of the MOPA was used to pump a large aperture (2mm x 2mm) PPMgLN based OPO producing 21 W of average output power at a slope efficiency of 45%. Up to 5.5 W of average power at a slope efficiency of 13% was obtained at the idler wavelength of 3.82 µm without thermal roll-off. Further enhancement in the OPO conversion efficiency should be possible using pulses with sub-nanosecond rise and fall times and operating the MOPA at 1030-1040 nm to mitigate short wavelength ASE build-up.

Acknowledgments

This work was supported in part by the UK Technology Strategy Board project SMART LASER, and was also partly supported by the National Natural Science Foundation of China (NSFC) (project 61078015), the National Basic Research Program (973) of China (project 2011CB311803).

#165617 - $15.00 USD Received 30 Mar 2012; revised 9 May 2012; accepted 6 Jun 2012; published 20 Jun 2012